Mechanical Evaluation of Na-Based Strain-Hardening Geopolymer Composites (SHGC) Reinforced with PVA, UHMWPE, and PBO Fibers

Ana C. C. Trindade[1(✉)], Iurie Curosu[2], Marco Liebscher[2], Viktor Mechtcherine[2], and Flávio de A. Silva[1]

[1] Department of Civil and Environmental Engineering, Pontifícia Universidade Católica Do Rio de Janeiro (PUC-Rio), Rio de Janeiro, RJ 22451-900, Brazil
ana.trindade@aluno.puc-rio.br
[2] TU Dresden, Institute of Construction Materials, 01062 Dresden, Germany

Abstract. Strain-hardening geopolymer composites (SHGC) show increased deformation capacity due to a multiple cracking tolerance under tensile loading. To evaluate their mechanical performance, a common metakaolin-based mixture was produced. Three types of short fibers were evaluated as disperse reinforcement: polyvinyl alcohol (PVA), ultra-high molecular weight polyethylene (UHMWPE), and poly(p-phenylen-2,6-benzobisoxazole) (PBO). The composites' mechanical features were analyzed in compression, three-point-bending, and tension tests with subsequent Environmental Scanning Electron Microscopy (ESEM) analysis of the fracture surfaces. Digital Image Correlation (DIC) was used to evaluate the extent of multiple cracking and crack widths under uniaxial tension. Additionally, single-fiber pullout tests were performed. PBO-based composites yielded the highest mechanical properties, reaching a 4.8 MPa peak stress in tension at a strain level of 2.3%, with a larger number of cracks. PVA and UHMWPE-based materials, however, demonstrated a lower mechanical performance, because of their larger diameter, lower mechanical properties and fiber-matrix adhesion.

Keywords: Geopolymer · SHGC · PVA · PE · PBO

1 Introduction

Strain-hardening geopolymer-based composites (SHGC) [1, 2] correspond to a class of materials known to result in a pronounced multiple cracking and high strain capacity under tensile loading, obtained by incorporating small amounts (~2% vol.) of synthetic micro-fibers into purposefully designed matrices [2, 3]. Their high inelastic deformability and excellent crack control makes a promising alternative for new constructions and retrofitting applications, also enhancing the performance of structures exposed to severe loading and environmental conditions [2]. The development of geopolymer-based composites occurred due to a demand for new alternative binders capable of enhancing the efficiency of strain-hardening cementitious composites

P. Serna et al. (Eds.): BEFIB 2021, RILEM Bookseries 36, pp. 857–867, 2022.
https://doi.org/10.1007/978-3-030-83719-8_73

(SHCC) [4, 5], both thermally and mechanically. This occurred since SHCC presents a relatively high amount of cement, due to strict limitations regarding aggregates' content [5], which can be highly associated with a significant CO_2 footprint [6, 7] as well as water demand, which is typical for cement-based mixtures [8]. Geopolymers [9] appear as an adequate alternative, due to their varied raw materials availability, mostly based on aluminosilicate binders mixed with alkali solutions [10, 11]. The "geopolymer" name was introduced by Davidovits [9], who established a binder based on aluminosilicate materials to enhance the thermal resistance of structural elements. Its empirical formula can be described as $M_2O{\bullet}Al_2O_3{\bullet}xSiO_2{\bullet}11H_2O$ (where M = Na, K, Cs; and x represents the Si/Al ratio used) [9]. The reaction and hardening processes, aside from the fast-setting time [12], enhanced thermal resistance [12], high chemical [13], and long-term durability [14], appear as suitable conditions in improving the long-term performance of the composites.

Various geopolymer-based composites have been investigated containing synthetic [15], mineral [16], and natural fabrics [14], as well as polymer micro-fibers [1–3, 17]. The latter approach was well explored by Nematollahi et al. [18] in studies on the production of fly ash based SHGC through a comprehensive analysis of the matrix and the establishment of optimal volume fractions of PE and PVA reinforcements. Additionally, Trindade et al. [1, 2] presented a complete mechanical evaluation of sand incorporation into KGP and NaGP metakaolin-based binders reinforced with PVA fibers, showing enhanced performance of the latter [1], and a PVA *versus* PE fibers comparison on the SHGC dynamic tensile behavior [2]. However, despite reaching reasonable tensile strength in the order of 4.5 MPa and adequate deformation values, further development can be designed by incorporating new and improved types of reinforcements, such as PBO fibers. Based on previous investigations on cementitious binders (SHCC) [19], this high-performance reinforcement is expected to result in superior mechanical properties [20], also exhibiting an improved behavior in high temperatures demands, which is in accordance with the geopolymer thermal capabilities [11].

Therefore, this study aims at a comprehensive evaluation of a well-established metakaolin-based geopolymer material (NaGP) concerning their use as a SHGC when reinforced with PVA, UHMWPE, and PBO fibers. The resulting mechanical performance characteristics are discussed based on compression, bending, uniaxial tension, pullout tests, and image observations (DIC and ESEM).

2 Experimental Program

2.1 Materials and Processing

The GP mixture was produced through the combination of Metamax metakaolin (MK) and an alkali-based solution (water glass, WG). Sodium hydroxide in pellets (reagent grade > 90%) was dissolved in deionized water, where hydrophilic fumed silica was added and mixed for 24 h using a magnetic stirrer, forming the stable water-glass solution. The WG-to-MK ratio was 1.71. Quartz fine sand (max. ϕ = 0.2 mm)

was incorporated in a 50% mass fraction of metakaolin. The MK chemical composition is presented in Table 1.

Table 1. MK chemical composition.

Composition	SiO_2	Al_2O_3	TiO_2	Fe_2O_3	K_2O	MgO	CaO	Na_2O	LOI
wt%	53.0	43.8	1.70	0.43	0.19	0.03	0.02	0.23	0.46

Short fibers 2% in vol. of PVA (Kuraray, Japan), UHMWPE (DSM, The Netherlands), and PBO (Toyobo, Japan) were used as reinforcements, with 12 mm lengths for the first two, and half of this value of the latter. Their physical and mechanical properties are presented in Table 2. A 10-L planetary mixer was used for the preparation of the composites as follows: (i) addition of metakaolin and water glass inside the mixer; (ii) mixing for 3 min at intermediate speed (198 rpm) to ensure adequate homogeneity and reactivity; (iii) addition of aggregates; (iii) mixing for 1 min at intermediate speed (198 rpm); (iv) addition of fibers; (v) mixing for 3 min at higher speed (365 rpm) ensuring a proper fiber distribution. The fresh mix was then poured into the molds, which required a vibration step of 1 min both for consolidation and removal of voids. The molds were sealed in plastic bags for 48 h at room temperature to prevent early dehydration [1, 2]. Subsequently, the samples were removed from the molds and cured inside dry plastic bags for 2 weeks, to prevent early dehydration.

Prismatic specimens of 160 mm × 40 mm × 40 mm were produced for the bending tests. Dumbbell-shaped specimens were produced for uniaxial tension tests, with a nominal cross-section in the gauge region of 40 mm × 24 mm.

Table 2. Physical and mechanical properties of the investigated PVA, UHMWPE, and PBO fibers

Fiber type	PVA (Kuralon® K-II REC15)	UHMWPE (Dyneema® SK62)	PBO-AS (Zylon®)
Length [mm]	12	12	6
Nominal diameter [μm]	40	20	13
Density [g/cm^3]	1.26	0.97	1.54
Tensile strength [MPa]	1600	2500	5800
Young's modulus [GPa]	40	80	180
Elongation at break [%]	7	3.5	3.5

The manufacturing process of single-fiber pullout specimens used a special rectangular polymer-made mold, allowing a longitudinal channel in the middle of the mold. The width of the channel corresponded to the fiber embedment length of 2 mm. The fibers were then transversely placed bridging the channel with a 10 mm-spacing between the fibers and carefully fixed with wax at their ends. The mold was subsequently filled with the fresh matrix. Demolding consisted of extracting the beams and

cutting between the fibers, resulting in at least 10 single specimens for each parameter variation. All shapes and geometries are presented in Fig. 1.

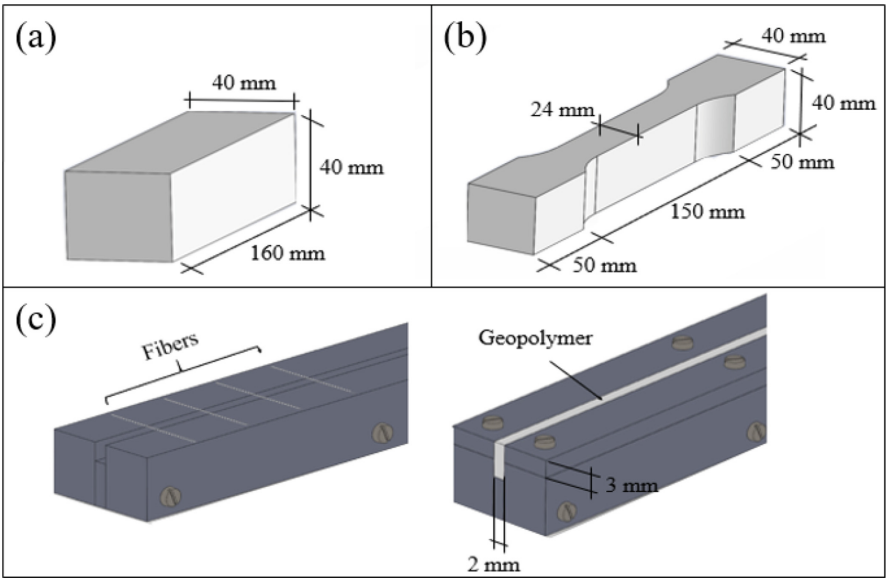

Fig. 1. Shapes and dimensions of (a) Prismatic specimen, (b) dumbbell-shaped specimen, and (c) mold and production of pullout specimens.

2.2 Testing Methods

A servo-hydraulic universal testing system with a load capacity of 200 kN was used to perform three-point bending tests with all material variations presented previously. The tests were carried out based on the BS EN 196-1 [21]; 3 specimens were tested for each variation under a load-controlled rate of 50 N/s. The span between supports was 100 mm.

Their compressive stress-deformation responses were obtained in the same testing system using 40 mm cubic samples, at a 2400 N/s loading rate. Hydraulic testing equipment Instron 8501 with closed-loop control and a load capacity of 100 kN was used to perform the uniaxial tension tests on the SHGC under a displacement rate of 0.04 mm/s. Three dumbbell-shaped specimens were tested for each composite variation. The specimens were glued at their ends in 20 mm-thick steel rings, bolted to the testing machine, ensuring non-rotatable boundary conditions. Two Linear Variable Differential Transducers (LVDTs) were placed on each side of the specimen using a steel frame to measure the deformation in a 100 mm gauge length. Figure 2a presents the testing configuration. During the tension tests, optical measurements were performed, to monitor and quantify the specimen's deformation and crack formation by using Digital Image Correlation (DIC). A black and white speckle pattern was sprayed

onto the specimens for this purpose. The optical sampling rate was 1 frame/5 s. The frames were processed with a commercial software ARAMIS 5M. Single-fiber pullout tests were performed for all three fiber-matrix combinations in an electromechanical testing machine Zwick 1445 with a 0.05 mm/s displacement rate using a 10 N capacity load cell. Figure 2b presents the testing configuration, with further details in a previous work [1]. The specimens were glued on a flat aluminum plate, which was screwed to the lower part of the machine. The free fiber end was glued to an upper plate, which was attached to the force sensor. Finally, an ESEM Quanta 250 FEG was used for microscopic analysis of the fracture surfaces of the GP fiber-reinforced composites.

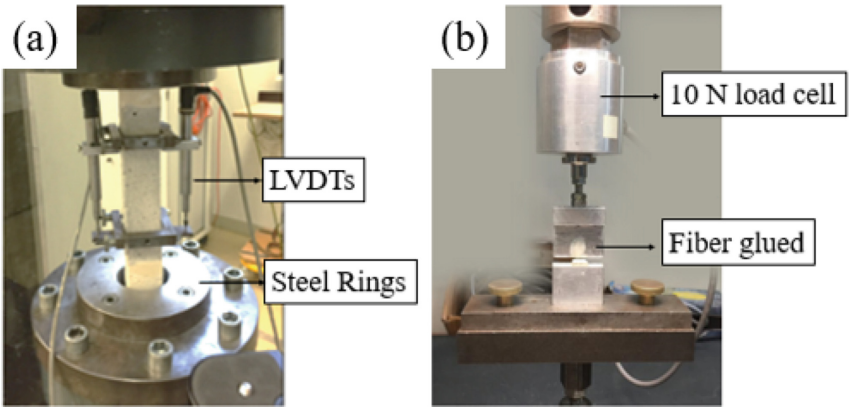

Fig. 2. (a) Uniaxial tension, and (b) pullout test configurations.

3 Results and Discussion

The compressive curves obtained with the plain sodium-based geopolymer (NaGP) material are presented in Fig. 3a, where it is possible to observe an average strength of 56.8 MPa and average Young's modulus of 9.6 GPa. Assuming that the effect of fibers is not substantial, these properties can be attributed to all composite variations since all of them were based on NaGP binders. The composites flexural curves obtained for the three types of SHGC reinforced with PVA, UHMWPE, and PBO fibers are shown in Fig. 3b, while the corresponding average mechanical parameters are summarized in Table 3.

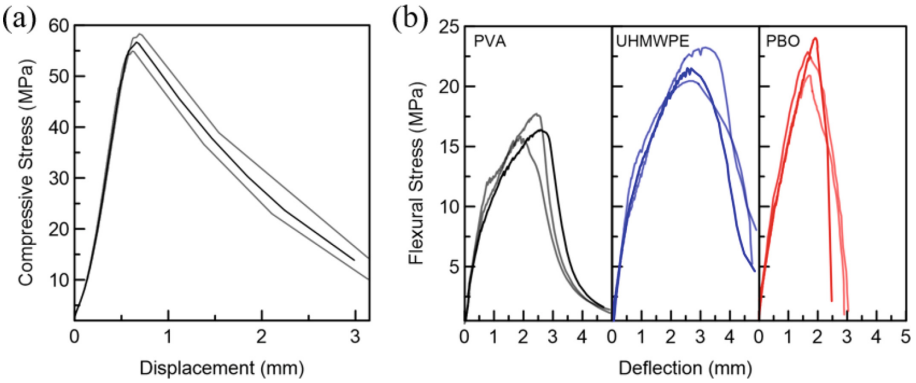

Fig. 3. (a) Compression and (b) three-point-bending tests results.

Table 3. Three-point-bending tests results.

Composite	$NaGP_{PVA}$	$NaGP_{PE}$	$NaGP_{PBO}$
First crack stress [MPa]	9.9 (1.1)	10.8 (0.7)	10.5 (0.5)
Flexural strength [MPa]	17.3 (0.9)	21.3 (1.1)	22.6 (1.4)
Deflection at peak stress [mm]	2.7 (0.2)	2.9 (0.4)	1.9 (0.1)
Work-to-fracture [N/mm]	27.3 (3.2)	40.5 (4.5)	26.5 (2.4)

All composites presented a ductile behavior with multiple cracks formations, due to efficient crack bridging by the micro-fibers. The three types of fibers acted as internal micro-confinements, enhancing the toughness and damage tolerance of the specimens. They all presented similar first crack stresses, reaching average 9.9, 10.8 and 10.5 MPa, for PVA, PE, and PBO reinforcements, respectively. This response is expected since the matrix properties rule the behavior of the composites in such elastic phase of loading (before cracking) [19]. Also, the slightly increased values found for PE and PBO reinforcements can be attributed to increased crack-bridging due to a smaller fiber diameter compared to PVA [1, 2]. Composites based on PBO fibers demonstrated an improved flexural strength of 22.6 MPa, followed by 21.3 and 17.3 MPa found for PE and PVA. This response is a direct result of the PBO fibers higher mechanical properties, and possibly fiber-matrix debonding mechanisms, even with half the length of PVA and PE filaments (6 mm for PBO). However, regarding maximum deflection and fracture energy, both PVA and PE fibers showed higher values, possibly indicating a greater crack opening for PVA and PE. This is also evidenced by the stress drops in the curves (not visible for PBO), characteristic of multiple crack formation, which will be further verified through DIC evaluations. To identify and properly quantify the effects of fiber type on the fiber-matrix interaction, single-fiber pullout tests appear to be instrumental.

The tensile behavior of NaGP composites reinforced with PVA, PE, and PBO fibers are presented in Fig. 4; Table 4 provides the average values obtained from the stress-strain curves.

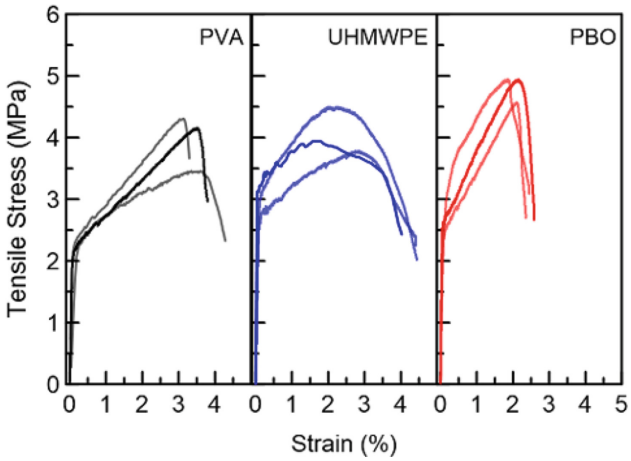

Fig. 4. Uniaxial tension tests results.

A pronounced enhanced first-crack stress can be distinguished for PE and PBO reinforcements when compared to PVA, reaching average 3.3, 3.1 and 2.9 MPa, respectively. This result could be expected in considering the previous flexural findings. Also, PBO-based composites demonstrated a superior mechanical capacity, reaching 4.8 MPa in stress, followed by 4.4 MPa with PE, and 4.2 MPa with PVA. An optimal balance between the cracking strength of the matrix and the crack-bridging capacity of the fibers was attained. The differences in fiber-matrix interactions for all types of matrices will be discussed when presenting the results of pullout tests. Regarding deformation values, it is possible to observe enlarged deformations for PVA and PE-based composites since they reached an average 3.2% of maximum deformation when compared to the 2.3% found for PBO. Again, no stress drops can be seen in the PBO curves, which can be associated with a controlled debonding in a low crack width. Therefore, the cracking parameters will be discussed through DIC evaluations in Fig. 5.

Table 4. Uniaxial tension tests results.

Composite	$NaGP_{PVA}$	$NaGP_{PE}$	$NaGP_{PBO}$
First crack stress [MPa]	2.9 (0.07)	3.3 (0.35)	3.1 (0.20)
Tensile stress [MPa]	4.2 (0.5)	4.4 (0.3)	4.8 (0.2)
Deformation at max. stress [%]	3.2 (0.8)	3.2 (0.7)	2.3 (0.2)
Fracture energy [N/mm]	8.1 (1.8)	8.9 (0.4)	10.7 (0.5)

The multiple cracking and fracture occurrence were evaluated, allowing the determination of the number of cracks, average crack width, and crack spacing. Figure 5 presents a typical analysis of the crack patterns at the final strain stage of

loading (2.3%), where most of the cracks have already been formed. A higher crack density was found for PBO-reinforced composites, when compared to the PVA and PE-based materials. The average crack widths recorded for PVA, PE, and PBO-based composites were: 64, 31, and 7 µm, respectively. The cracks found in PBO-based composites were narrower than in PVA and PE. It is interesting to notice the slightly better crack control in comparison to common SHCC, which typically yields increased crack widths and crack spacings in stronger matrices [23, 24].

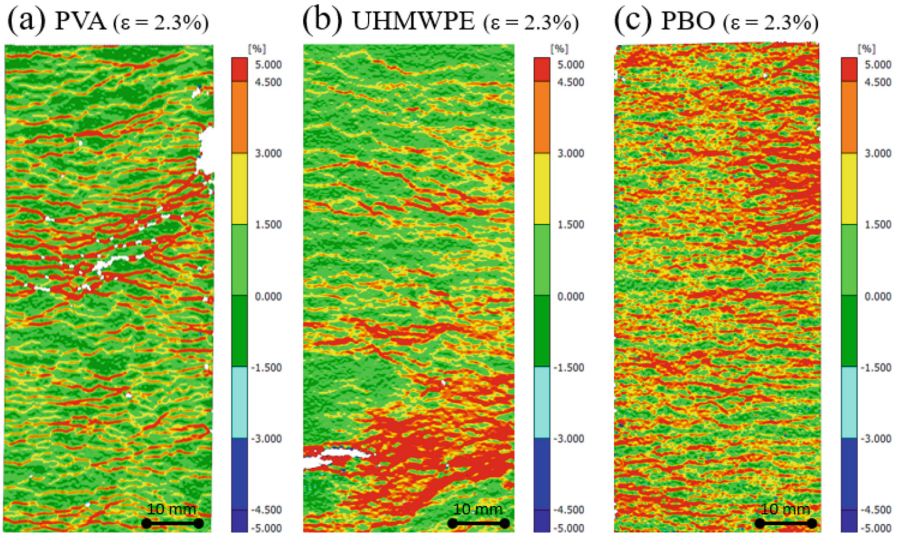

Fig. 5. DIC analysis – cracking evaluation, for representative (a) PVA, (b) UHMWPE, and (c) PBO fiber-reinforced NaGP.

The pullout test results are presented in Fig. 6 and Table 5. All fibers demonstrated a complete fiber pullout, which is indicated by the relatively steady and long descending branches of force-displacement curves. Opposed to the interfacial damage usually recorded in common PVA-SHCC materials [22], the pullout of the PVA fibers from NaGP resulted in a slip-softening behavior, indicating a dramatic reduction of the chemical adhesion through binder substitution. Also, it is interesting to notice a great difference for the bond strength values found for PBO reinforcements, 2.36 MPa, when compared to 0.94 and 0.81 MPa reached with PVA and PE. This enhancement is associated with the fiber's improved mechanical properties in a similar embedment pullout length (2 mm), contributing also to the composites crack bridging, justifying the slightly greater flexural and tensile load-bearing capacities found previously, even with half the length compared to the other two reinforcements. The latter being the main responsible for the small improvements in stress, when compared to the 12 mm lengths of both PVA and PE reinforcements.

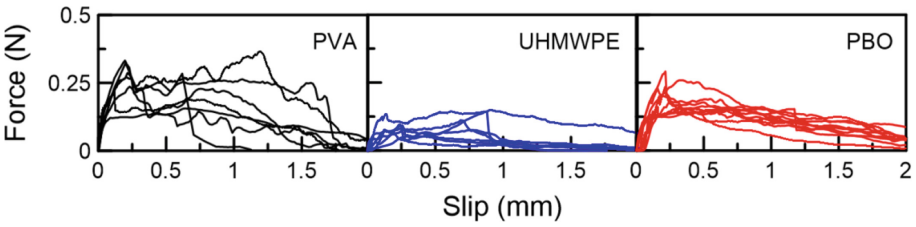

Fig. 6. Pullout tests results for (a) PVA, (b) UHMWPE, and (c) PBO fibers.

Table 5. Pullout tests results.

Fiber	PVA	UHMWPE	PBO
Peak force [N]	0.23 (0.06)	0.10 (0.03)	0.19 (0.08)
Bond strength [MPa]	0.94 (0.22)	0.81 (0.14)	2.36 (0.69)

Figure 7 presents the fracture surfaces of all three composites, showing the surfaces of the partially pulled out fibers after complete failure in the uniaxial tension tests, without any evident fiber surface damage. Micrographs also revealed some regions of fiber agglomerations, especially for PE reinforcements, due to its increased number of filaments, when compared to the same PVA fiber content, evidencing a need for rheological and mixing optimizations. The images clearly show the differences in fiber diameters, and the high homogeneity of the NaGP matrix and its pronounced brittleness, marked by the fine loose fragments.

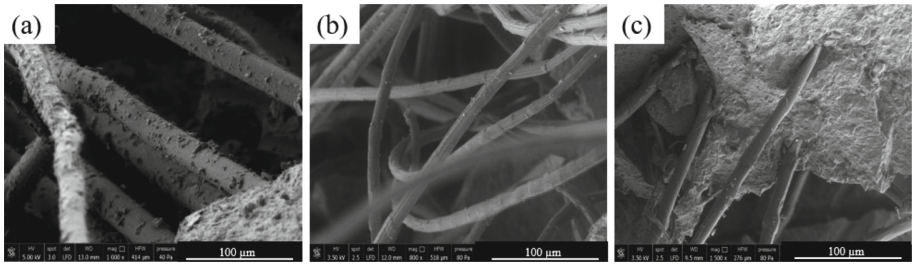

Fig. 7. Fracture surfaces of (a) PVA, (b) UHMWPE, and (c) PBO fiber reinforced NaGP.

Therefore, these results demonstrate the superior crack-bridging behavior of the PBO fibers, evidenced by the composites' ability to withstand higher loads, showing further developments for the SHGC technology, allowing the use of varied fibers into a well-known geopolymer binder for a varied range of applications, such as retrofit in elements subjected to dynamic loading and possibly requiring long-term durability.

4 Conclusions

The results of the experimental investigations showed that PBO-based composites mixtures exhibited higher tensile and flexural strengths when compared to the same PVA and UHMWPE variations. In general, the fibrous reinforcement was effective in ensuring typical strain-hardening behavior under tensile loading, accompanied by pronounced multiple cracking. PBO-based strain-hardening geopolymer composites (SHGC) yielded strain capacities of 2.3% and tensile stresses of 4.8 MPa, while the same PVA and UHMWPE achieved only 4.4 and 4.2 MPa on average.

Pullout tests made possible a comprehensive analysis of the fiber-matrix interactions, evidencing a stronger fiber anchorage for PBO-based composites, reaching a considerably higher bond strength of 2.36 MPa. In contrast, PVA and UHMWPE-based composites showed weaker bonds, which led to larger crack openings, also enhancing their ultimate deformations. DIC evaluations of crack formation showed that the PBO-based SHGC exhibited average crack widths of 7 μm, while PVA and UHMWPE variations exhibited 64 μm and 7 μm, respectively, because of the stronger bond, higher fiber stiffness and smaller diameter.

In summary, improved strain capacity and smoother shape of the stress-strain curves were observed for SHGCs produced with PBO reinforcements. However, despite the higher stresses, more abrupt failure modes were found, showing that it could be relevant to combine PBO with PE fibers in future works and applications. This indicates further potential for the development of SHGC materials for a wide range of applications, including structural elements subject to dynamic loading.

Acknowledgements. The authors acknowledge the financial support provided by the Brazilian organizations CNPq and CAPES (Probral project number 8887.144079/2017-00) and by the DAAD program (Probral project number 8887.144079/2017-00) in Germany. Also, the use of the facilities at the TU Dresden and the support of the laboratory staff at the Institute of Construction Materials are greatly appreciated.

References

1. Trindade, A.C.C., Curosu, I., Liebscher, M., Mechtcherine, V., de Andrade Silva, F.: On the mechanical performance of K-and Na-based strain-hardening geopolymer composites (SHGC) reinforced with PVA fibers. Constr. Build. Mater. **248**, 118558 (2020)
2. Trindade, A.C.C., Heravi, A.A., Curosu, I., Liebscher, M., de Andrade Silva, F., Mechtcherine, V.: Tensile behavior of strain-hardening geopolymer composites (SHGC) under impact loading. Cem. Concr. Compos. **113**, 103703 (2020)
3. Batista, R.P., Trindade, A.C.C., Ribeiro Borges, P.H., Silva, F.A.: Silica fume as precursor in the development of sustainable and high-performance MK-based alkali-activated materials reinforced with short PVA fibres, Front. Mater. **6**(77) (2019)
4. Mechtcherine, V.: Novel cement-based composites for the strengthening and repair of concrete structures. Constr. Build. Mater. **41**, 365–373 (2013)
5. Choi, W.C., Yun, H.D., Kang, J.W., Kim, S.W.: Development of recycled strain-hardening cement-based composite (SHCC) for sustainable infrastructures. Compos. B Eng. **43**(2), 627–635 (2012)

6. Li, V.: Sustainability of engineered cementitious composites (ECC) infrastructure. In: Engineered Cementitious Composites (ECC) Bendable Concrete for Sustainable and Resilient Infrastructure, pp. 261–312. Springer, Heidelberg (2019). https://doi.org/10.1007/978-3-662-58438-5_8
7. Schneider, M., Romer, M., Tschudin, M., Bolio, H.: Sustainable cement production—present and future. Cem. Concr. Res. **41**(7), 642–650 (2011)
8. Shi, C., Jiménez, A.F., Palomo, A.: New cements for the 21st century: the pursuit of an alternative to Portland cement. Cem. Concr. Res. **41**(7), 750–763 (2011)
9. Davidovits, J.: Geopolymers: inorganic polymeric new materials. J. Therm. Anal. Calorim. **37**(8), 1633–1656 (1991)
10. Purdon, A.O.: The action of alkalis on blast-furnace slag. J. Soc. Chem. Indust. **59**(9), 191–202 (1940)
11. Vickers, L., Van Riessen, A., Rickard, W.D.: Fire-Resistant Geopolymers: Role of Fibres and Fillers to Enhance Thermal Properties. Springer, Singapore (2015). https://doi.org/10.1007/978-981-287-311-8
12. Kriven, W.M., Bell, J.L., Gordon, M.: Microstructure and microchemistry of fully-reacted geopolymers and geopolymer matrix composites. Ceram. Trans. **153**, 227–250 (2003)
13. Provis, J.L., Van Deventer, J.S.J.: Geopolymers: Structures, Processing, Properties and Industrial Applications. Elsevier, Amsterdam (2009)
14. Trindade, A.C.C., Alcamand, H.A., Borges, P.H.R., Silva, F.A.: On the durability behaviour of natural fiber reinforced geopolymers. Ceram. Sci. Proc. **38**(3), 215–228 (2017)
15. Menna, C., et al.: Use of geopolymers for composite external reinforcement of RC members. Compos. B Eng. **45**(1), 1667–1676 (2013)
16. Dias, D.P., Thaumaturgo, C.: Fracture toughness of geopolymeric concretes reinforced with basalt fibers. Cem. Concr. Compos. **27**(1), 49–54 (2005)
17. Nematollahi, B., Sanjayan, J., Ahmed Shaikh, F.U.: Tensile strain hardening behaviour of PVA fiber-reinforced engineered geopolymer composite. J. Mater. Civil Eng. **27**(10), 04015001 (2015)
18. Nematollahi, B., Sanjayan, J., Qiu, J., Yang, E.H.: Micromechanics-based investigation of a sustainable ambient temperature cured one-part strain hardening geopolymer composite. Constr. Build. Mater. **131**, 552–563 (2017)
19. Curosu, I., Liebscher, M., Mechtcherine, V., Bellmann, C., Michel, S.: Tensile behavior of high-strength strain-hardening cement-based composites (HS-SHCC) made with high-performance polyethylene, aramid and PBO fibers. Cem. Concr. Res. **98**, 71–81 (2017)
20. Gong, T., Heravi, A., Alsous, G., Curosu, I., Mechtcherine, V.: The impact-tensile behavior of cementitious composites reinforced with carbon textile and short polymer fibers. Appl. Sci. **9**(19), 4048 (2019)
21. BS EN 196-1: Methods of Testing Cement. Part 1: Determination of Strength (2016)
22. Barbosa, V.F., MacKenzie, K.J.: Thermal behaviour of inorganic geopolymers and composites derived from sodium polysialate. Mater. Res. Bull. **38**(2), 319–331 (2003)
23. Van Zijl, G.P.A.G., Wittmann, F.H.: Durability of Strain-Hardening Fibre-Reinforced Cement-Based Composites (SHCC), vol. 4. Springer, Heidelberg (2010). https://doi.org/10.1007/978-94-007-0338-4
24. Curosu, I., et al.: Influence of fiber type on the tensile behavior of high-strength strain-hardening cement-based composites (SHCC) at elevated temperatures. Mater. Des. **198**, 109397 (2020)